Наносистеми, наноматеріали, нанотехнології
Nanosistemi, Nanomateriali, Nanotehnologii
2020, т. 18, № 1, сс. 53–58

© 2020 ІМФ (Інститут металофізики
ім. Г. В. Курдюмова НАН України)
Надруковано в Україні.
Фотокопіювання дозволено
тільки відповідно до ліцензії

PACS numbers: 61.72.Ff, 61.72.Mm, 68.35.Ct, 68.37.Ps, 68.55.J-, 81.15.Cd, 81.15.Gh

Morphology of Thin Films Y_2O_3:Eu Obtained by Different Methods

O. M. Bordun[1], I. O. Bordun[1], I. M. Kofliuk[1], I. Yo. Kukharskyy[1],
I. I. Medvid[1], Zh. Ya. Tsapovska[1], and D. S. Leonov[2]

[1]*Ivan Franko National University of Lviv,*
50, Drahomanov Str.,
UA-79005 Lviv, Ukraine
[2]*Technical Centre, N.A.S. of Ukraine,*
13, Pokrovska Str.,
UA-04070 Kyiv, Ukraine

Thin Y_2O_3:Eu films are obtained by the method of radio-frequency (RF) ion-plasma sputtering in an argon atmosphere and discrete evaporation in vacuum. Investigation of the surface morphology of thin films by atomic force microscopy (AFM) shows that, when switching from RF sputtering to discrete evaporation, the mean square surface roughness increases at close diameters of nanocrystallite grains on the film surface. As established, the grain-size distribution during RF sputtering corresponds to the normal logarithmic distribution with one distribution centre, and for discrete evaporation, this is with two distribution centres. The ratio of distribution centres indicates the coalescence of grains with themselves.

Методою високочастотного (ВЧ) йонно-плазмового розпорошення в атмосфері арґону та дискретного випаровування у вакуумі одержано тонкі плівки Y_2O_3:Eu. Дослідження морфологій поверхні тонких плівок методою атомно-силової мікроскопії (АСМ) показало, що при переході від ВЧ-розпорошення до дискретного випаровування зростає середня квадратична шерсткість поверхні за близьких величин діяметрів нанокристалічних зерен на поверхні плівок. Встановлено, що розподіл зерен за діяметром при ВЧ-розпорошенні відповідає нормальному логаритмічному розподілу з одним центром розподілу, а при дискретному випаровуванні — з двома центрами розподілу. Співвідношення центрів розподілу вказує на зрощування зерен між собою.

Методом высокочастотного (ВЧ) ионно-плазменного распыления в атмосфере аргона и дискретного испарения в вакууме получены тонкие плёнки Y_2O_3:Eu. Исследование морфологи поверхности тонких плёнок методом атомно-силовой микроскопии (АСМ) показало, что при перехо-

де от ВЧ-распыления к дискретному испарению возрастает средняя квадратическая шероховатость поверхности при близких величинах диаметров нанокристаллических зёрен на поверхности плёнок. Установлено, что распределение зёрен по диаметру при ВЧ-распылении соответствует нормальному логарифмическому распределению с одним центром распределения, а при дискретном испарении — с двумя центрами распределения. Соотношение центров распределения указывает на срастание зёрен между собой.

Key words: yttrium oxide, thin films, nanocrystallite.

Ключові слова: оксид ітрію, тонкі плівки, нанокристаліти.

Ключевые слова: оксид иттрия, тонкие плёнки, нанокристаллиты.

(Received 28 January, 2020)

1. INTRODUCTION

Significant interest in the study of nanostructures of various chemical composition, structure and morphology caused by interesting physicochemical, electrical, optical and other properties of nanomaterials, which open up broad prospects for their practical application [1–3]. Among them, a special place is occupied by materials doped with rare-earth ions (REI), which are key elements of modern devices for generating, transmitting, and controlling optical signals. One of the most used REIs is europium Eu^{3+}, which is widely used in nuclear power, to generate laser radiation in the visible spectrum with a wavelength of 0.61 μm, and $Y_2O_3:Eu^{3+}$ is the most efficient phosphor emitting in the red spectrum [4–6]. The combination of small sizes of crystalline particles and the presence of dopants as luminescent centres, *i.e.*, ions of rare-earth metals, provides high efficiency and stability of the luminescence of such materials, expanding their potential areas of application. An analysis of the size, morphological, and structural characteristics of nanoparticles suggests that they largely depend on the method and conditions for producing nanostructures [7–9]. This led to the study of the surface morphology of thin $Y_2O_3:Eu^{3+}$ films obtained by radio-frequency (RF) ion-plasma sputtering and discrete thermal evaporation in vacuum. Among the high-precision methods in determining the size and morphology of nanoparticles include atomic force microscopy (AFM), which was used in this work.

2. EXPERIMENTAL TECHNIQUE

Thin films of $Y_2O_3:Eu$ with a thickness of 0.2–1.0 μm were obtained

by RF ion-plasma sputtering and discrete evaporation in vacuum on fused υ-SiO_2 quartz substrates. RF sputtering was carried out in an argon atmosphere in a system using the magnetic field of external solenoids for compression and additional ionization of the plasma column. The feedstock was Y_2O_3 grade ИтО-И and Eu_2O_3 with grade «ос.ч». The activator concentration was 1 mol.%. After deposition of the films, the heat treatment in air at 950–1050°C was held.

Using the x-ray diffraction analysis (Shimadzu XDR-600), the structure and phase composition of the films were studied. X-ray diffraction studies showed the presence of a polycrystalline structure with a predominant orientation in the (222) plane. The form of the obtained diffraction patterns is almost analogous to the diffraction patterns of pure Y_2O_3 films that we presented in [10]. All diffraction maxima are identified according to the selection rules and belong to the space group $T_h^7 = Ia^3$, which indicates the cubic structure of the obtained films.

The surface morphology of films was investigated using an atomic force microscope (AFM) 'Solver P47 PRO'. Processing of experimental data and calculation of surface morphology parameters was carried out using the Image Analysis 2 software package.

3. RESULTS AND DISCUSSION

Microphotographs of the surface of Y_2O_3:Eu films obtained by RF sputtering and discrete evaporation obtained using AFM are shown in Fig. 1.

The topography of the samples was quantitatively characterized by standard parameters: root mean square roughness, maximum grain height with diameter and grain height, which were calculated according to AFM data for sections of the same size (1000×1000 nm). The characteristic parameters of thin films Y_2O_3:Eu obtained by various methods are listed in Table.

The analysis of AFM images (Fig. 1) and parameters of crystalline grains (Table) of the surface of Y_2O_3:Eu films shows that, upon transition from RF sputtering to discrete evaporation, the root mean square surface roughness and the maximum grain height increase. An increase in the root mean square roughness parameter indicates a complication of the surface structure. A comparison of the histograms of the distribution of heights (Fig. 2) shows that, when switching from RF, sputtering into discrete evaporation leads to the formation of sharper peaks on the film surface.

A slight decrease in the grain concentration and a simultaneous increase in grain sizes in thin films Y_2O_3:Eu upon transition from RF-sputtering into discrete evaporation (Table) indicate the possibility of the surface transition of the Y_2O_3:Eu film upon discrete evap-

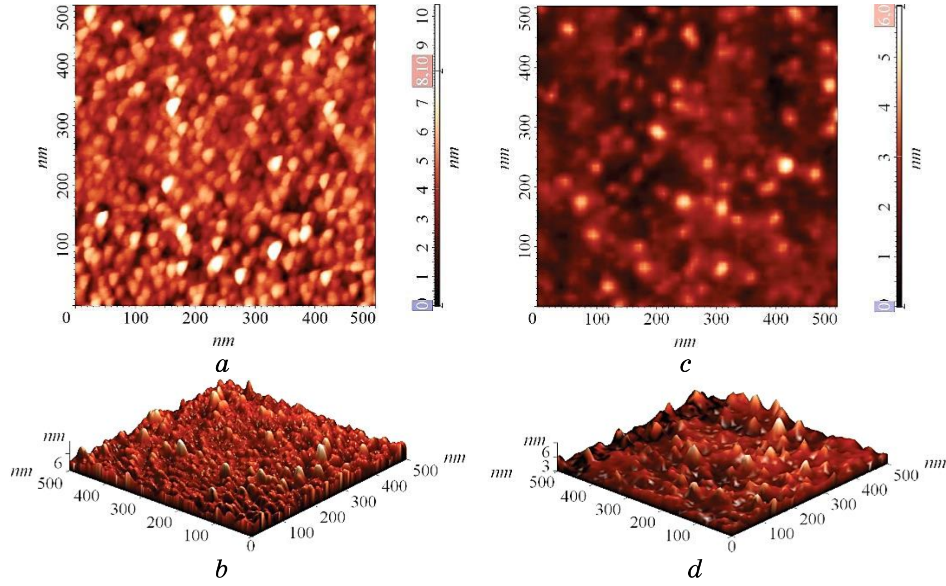

Fig. 1. Images of the surface morphology of a thin film Y_2O_3:Eu obtained by RF sputtering (*a*, *b*) and discrete evaporation (*c*, *d*). Image *a* and *c* are two-dimensional, *b* and *d* are three-dimensional.

TABLE. Parameters of crystallite grains of Y_2O_3:Eu thin films.

Parameter	RF-sputtering	Discrete evaporation
Grains diameter, nm	15.7	15.7
Root mean square roughness, nm	0.7	1.2
Max height grains, nm	6.0	10.3
Grains volume, nm^3	1123.5	1469.5

oration to a more nanostructured state due to crystallization of the surface layer.

In general, it was found that the grain size distribution is fairly well described by the normal logarithmic law typical for polycrystalline materials [11]:

$$f(d) = \frac{1}{\sigma d\sqrt{2\pi}} e^{-[\ln d - \mu]^2/2\sigma^2},$$

where d is the grain diameter, σ is the standard deviation (dispersion) of $\ln d - \mu$, μ is the average value of $\ln d$.

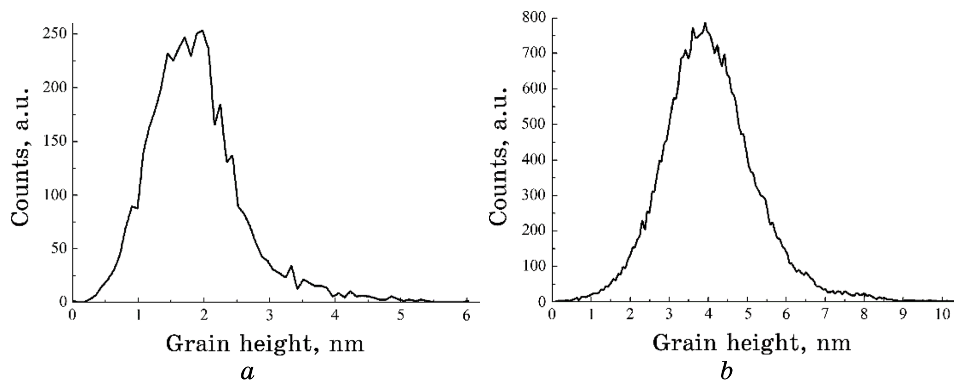

Fig. 2. Grain height distribution on an AFM image of thin films Y_2O_3:Eu obtained by RF sputtering (*a*) and discrete evaporation (*b*).

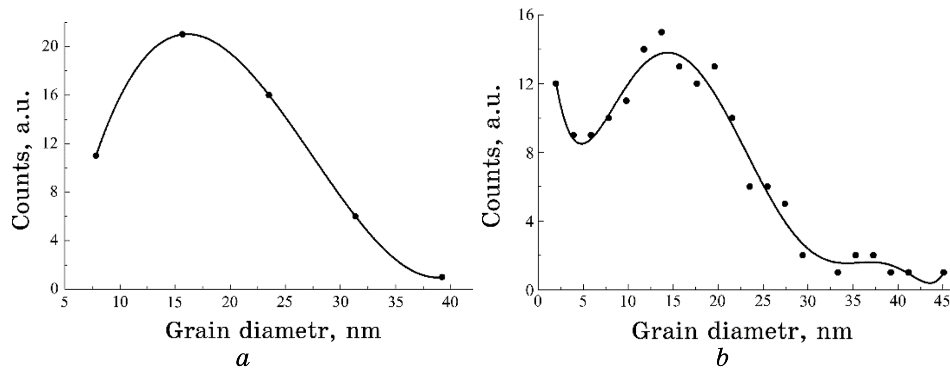

Fig. 3. Distribution of grain diameter sizes and calculated approximation of the diameter distribution on AFM images of Y_2O_3:Eu thin films obtained by RF sputtering (*a*) and discrete evaporation (*b*).

The larger grain growth of the Y_2O_3:Eu film during discrete sputtering relative to RF sputtering leads to the appearance of additional maxima in the calculated diameter distribution of grains in AFM images (Fig. 3).

The analysis shows that, for the surface of films during RF sputtering, one division is observed in diameter with a maximum of about 16 nm and a dispersion of 3 nm, and with discrete evaporation, at least two distributions with maxima of about 16 and 36 nm and a dispersion of 3.3 and 3.0 nm, respectively, and a certain increase in the number of grains in the region of small diameters. Since the centres of the obtained distributions are fairly closely related as integers 1:2, this indicates a certain intergrowth of small grains with the formation of large ones.

4. CONCLUSIONS

It has been established that, during RF ion-plasma sputtering and discrete evaporation, polycrystalline Y_2O_3:Eu films consisting of nanometer grains are formed. According to AFM data, it is shown that, upon transition from RF sputtering to discrete evaporation, the mean square surface roughness increases, although the average grain diameter on the film surface in both cases is 15.7 nm. In this case, the diameter distribution of grains during RF sputtering corresponds to the normal logarithmic distribution with one distribution centre, and for discrete evaporation, this is with two distribution centres, which approximately correlate as 1:2 that indicates grain coalescence.

REFERENCES

1. K. M. Nissamudeen and K. G. Gopchandran, *J. Alloys and Compounds*, **490**: 399 (2010).
2. P. Packiyaraj and P. Thangadurai, *J. Luminescence*, **145**: 997 (2014).
3. H. Huang, G. A. Xu, W. S. Chin, and L. M. Gan, *Nanotechnology*, **13**, No. 3: 318 (2002).
4. C. Shanga, X. Shang, Y. Qu, and M. Li, *Chem. Phys. Lett.*, **501**, Nos. 4–6: 480 (2011).
5. O. M. Bordun, I. O. Bordun, I. Yo. Kukharskyy, Zh. Ya. Tsapovska, and M. V. Partyka, *J. Appl. Spectrosc.*, **84**, No. 6: 1072 (2018).
6. H. M. Abdelaal, A. Tawfik, and A. Shaikjee, *Mater. Chem. Phys.*, **242**: 122530 (2020).
7. Hai Guo and Yan Min Qia, *Opt. Materials*, **31**, No. 3: 583 (2009).
8. O. M. Bordun and I. M. Bordun, *Optika i Spektroskopiya*, **88**, No. 5: 775 (1997).
9. L. Wen, X. Sun, Q. Lu, and G. Xu, *Opt. Mater.*, **29**: 239 (2006).
10. O. M. Bordun, I. O. Bordun, and I. Yo. Kukharskyy, *J. Appl. Spectrosc.*, **82**, No. 3: 390 (2015).
11. J. E. Palmer, C. V. Thompson, and H. I. Smith, *J. Appl. Phys.*, **62**, No. 6: 2492 (1987).